DOI: 10.1002/ejic.200600550

Cu/Zn/Al Xerogels and Aerogels Prepared by a Sol–Gel Reaction as Catalysts for Methanol Synthesis

Yanzhi Guo,[a] Wolfgang Meyer-Zaika,[a] Martin Muhler,[b] Sascha Vukojević,[c] and Matthias Epple*[a]

Keywords: Heterogeneous catalysis / Copper / Zinc / Aluminum / Sol–gel processes / Mesoporous materials

ZnO/Al_2O_3, CuO/Al_2O_3, and $CuO/ZnO/Al_2O_3$ xerogels and aerogels have been prepared by a sol–gel route using propylene oxide as gelation initiator. For aerogel preparation, the solvent was extracted with supercritical CO_2. Calcination of these xerogels and aerogels was followed by thermogravimetry (TG), and the microstructure of these calcined xerogels and aerogels was investigated by TEM, powder XRD, EXAFS, and nitrogen physisorption (BET, BJH). The oxide mixtures CuO/Al_2O_3 and $CuO/ZnO/Al_2O_3$ were also studied by temperature-programmed reduction (TPR), and their catalytic activity in the formation of methanol from $CO/CO_2/H_2$ synthesis gas was measured. The aerogels have a higher specific surface area and a higher Cu surface area than the corresponding xerogels, which results in a higher catalytic activity for methanol synthesis. The presence of ZnO significantly increases the catalytic activities of both the xerogel and the aerogel.

Introduction

$Cu/ZnO/Al_2O_3$ catalysts are widely used for the industrial synthesis of methanol, for methanol reforming, and for the water-gas shift reaction, and have therefore been intensively investigated in the last few decades.[1–3] Various methods have been developed for the preparation of $Cu/ZnO/Al_2O_3$ catalysts. The differences in preparation methods, synthesis conditions, and pre-treatment have a considerable influence on the structure of the catalysts, which finally leads to disparities in the catalytic performance. It is generally accepted that a large specific Cu surface area leads to an active methanol synthesis catalyst.[1,4] In addition, the metal–support interaction plays a key role in this catalytic reaction.[1,2,5,6]

Catalyst preparation usually involves complex processes and the performance of the final product is very sensitive to rather subtle changes in the synthetic procedures.[7–11] Copper/zinc oxide nanocomposites are usually prepared by co-precipitation from aqueous solutions. Typically, a mixed solution of copper and zinc salts (frequently nitrates or acetates) is prepared and the precipitation of both carbonates is induced by the addition of sodium or ammonium carbonate whilst stirring, followed by drying and calcination.[8,9,12] The particle size and crystallinity of the products can be adjusted by varying the pH, the reactant concentrations, the stirring rate, the duration of precipitation and aging, and the calcination conditions.[13] Günter et al. have investigated binary Cu/ZnO catalysts with varying Cu/Zn molar ratios (90:10 to 10:90) and found that the precursor phase composition directly influences the resulting Cu microstructure and, in turn, the performance of the Cu/ZnO catalyst.[8] The effect of pH on the composition of the precursors and the activity of the $Cu/ZnO/Al_2O_3$ catalysts for methanol synthesis has been studied by Fang et al.,[14] and Deng et al. have prepared ultra-fine $Cu/ZnO/Al_2O_3$ catalysts by an oxalate gel co-precipitation.[15] The obtained catalysts show a high activity in methanol synthesis. A non-aqueous organometallic route has been developed by Fischer et al. and uniform copper/zinc nanoparticles ("nanobrass") were obtained with $[Cu\{OCH(Me)CH_2NMe_2\}_2]$ and Et_2Zn as precursors.[16] Schüth et al. have reported that colloidal copper nanoparticles prepared by reduction of copper acetylacetonate with trialkylaluminum are highly active for quasi-homogeneous methanol synthesis.[17] We have reported the preparation of copper/zinc nanocomposites by the thermolysis of dimetallic copper/zinc cyanide coordination compounds under mild conditions.[18–21] For instance, the copper/zinc cyanide compound $[Zn\{Cu(CN)_3\}]$ was precipitated by both a batch-wise and a continuous synthesis method. Depending on the ligands in the complex and the thermolysis conditions, the activity towards methanol synthesis could be controlled.[21]

The sol–gel route can be considered as a very interesting way of preparing catalysts because of the possibility to con-

[a] Inorganic Chemistry, University of Duisburg–Essen, Universitaetsstrasse 5–7, 45117 Essen, Germany
Fax: +49-201-183-2621
E-mail: matthias.epple@uni-due.de
[b] Laboratory of Industrial Chemistry, Ruhr University Bochum, Universitaetsstrasse 150, 44801 Bochum, Germany
[c] Max-Planck-Institute for Coal Research, Kaiser-Wilhelm-Platz 1, 45470 Muelheim an der Ruhr, Germany

trol many variables involved in the synthesis.[22] Traditionally, the sol–gel method has involved the use of metal alkoxide precursors that readily undergo catalyzed hydrolysis and condensation to form a sol of metal oxide particles with nanoscale dimensions (1–100 nm).[22] This route has proven to be an efficient, easy, and successful approach for the preparation of SiO_2-, Al_2O_3-, and ZrO_2-based porous materials.[23] A novel sol–gel technique was recently developed for the preparation of transition and main-group metal oxide aerogels, xerogels, and nanocomposites.[24] This method involves the use of epoxides as gelation initiators in the preparation of porous metal oxides such as Fe_2O_3, Al_2O_3, and Cr_2O_3.[25,26] Here we report the sol–gel preparation and catalytic performance of Cu-, Zn-, and Al-based di- and trimetallic nanocomposites by this method.

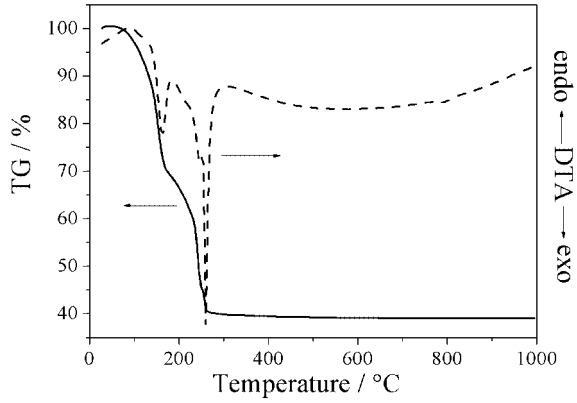

Figure 1. TG and DTA analysis of the Cu/Zn/Al dried xerogel (1:1:1) under dynamic oxygen atmosphere (5 $K\,min^{-1}$), leading to an intimate mixture of CuO, ZnO, and Al_2O_3.

Results and Discussion

Synthesis

Metal oxide aerogels and xerogels can be prepared directly from metal salts using epoxides as gelation initiators.[27,28] These initiators, which act as irreversible proton scavengers, induce the hydrolysis and condensation of hydrated metal cations. The initiators consume the protons from the hydrated metal species and enhance the sol–gel condensation reaction. The protonated epoxide is ultimately consumed during gelation by a ring-opening reaction with a suitable nucleophile. In this work, propylene oxide was used as gelation initiator and the gel formed within 30–60 min in ethanol solution. No shrinkage was observed either during the gelation process or in the drying process with supercritical carbon dioxide. However, shrinkage was observed after drying in air to a xerogel. As a result, the obtained oxide xerogels and aerogels exhibit very low densities, especially the latter. Different combinations of metals were realized.

Thermolysis of the Zn/Al and Cu/Zn/Al Xerogels and Aerogels

The thermal decomposition of the air-dried xerogels and the aerogels to the corresponding oxides was studied by thermogravimetry (TG).[29] The decomposition behavior showed only a small dependence on the composition of the gel, i.e. the ratio of Cu/Zn/Al or the drying procedure (air-drying or extraction with supercritical CO_2). Figure 1 shows the TG and DTA curves of a Cu/Zn/Al air-dried xerogel (1:1:1) under dynamic oxygen atmosphere. The first peak is a broad endothermal one with a maximum at about 92 °C, which is probably due to the loss of residual volatile solvent (ethanol or water). The subsequent exothermal peaks at 160, 245, and 260 °C can be attributed to the oxidation of residual organic compounds, which is in good agreement with the literature.[28] The total weight loss is about 60%. A similar behavior has been observed for the other samples, although with slight temperature variations of the exothermal peaks.

ZnO/Al_2O_3 Xerogels

TEM images of the calcined ZnO/Al_2O_3 xerogel with different Zn/Al ratios are shown in Figure 2. The particles in Figure 2a have a typical particle diameter of 10 nm. When the Zn/Al ratio was increased to 2:1, the homogeneity decreased, with particle sizes up to 30 nm (Figure 2b).

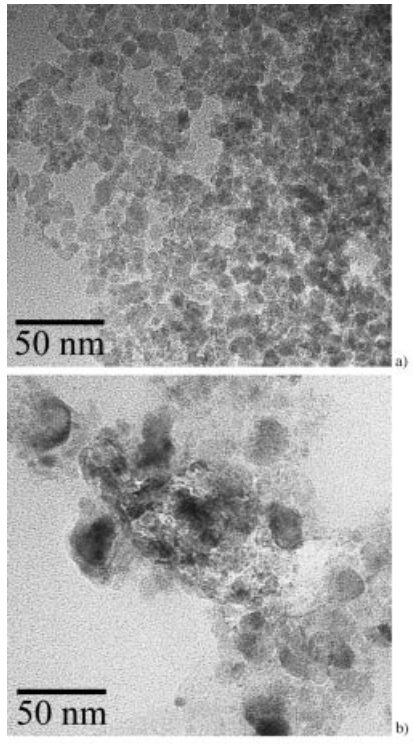

Figure 2. TEM images of ZnO/Al_2O_3 calcined xerogels (400 °C) with different Zn/Al molar ratios: a) Zn/Al = 1:2; b) Zn/Al = 2:1.

The structure of the sol–gel products depends on the type and concentration of the polyoxometalates present during the formation of the condensed gel.[26] The nature of these

transient species is determined by a number of synthesis parameters, such as the reaction pH, solvent, temperature, ionic strength of the solution, as well as the compositions in the case of mixed species. XRD studies showed that the crystallinity of the Zn/Al oxides is strongly affected by the Zn/Al ratio (Figure 3). ZnO/Al_2O_3 is X-ray amorphous for a Zn/Al ratio of 1:2, thus indicating the absence of long-range order. However, for a 2:1 ratio the crystallinity increases significantly, as indicated by peaks originating from ZnO nanocrystals corresponding to the presence of larger particles in the TEM image. The Al_2O_3 phase is always X-ray amorphous.

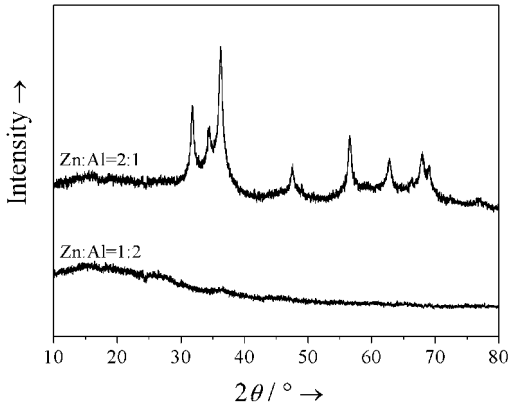

Figure 3. XRD patterns of ZnO/Al_2O_3 calcined xerogels (400 °C) with different Zn/Al molar ratio. All peaks in the upper diffractogram correspond to ZnO.

A closer look at the structure of the ZnO/Al_2O_3 calcined xerogel (400 °C) was obtained by EXAFS (Figure 4 and Table 1). In the Zn K-edge Fourier transform magnitudes, the first shell of Zn–O in ZnO is clearly present in both samples. The Zn–Zn shells at about 3 Å, however, are different for different Zn/Al ratios. For the sample with a Zn/Al ratio of 1:2 the Zn–Zn peak is almost invisible. The absence of Zn neighbors around Zn suggests a high structural disorder or a dispersion of ZnO in Al_2O_3 on the atomic scale. This dispersion can be beneficial when these ZnO/Al_2O_3 oxide mixtures are used as a support for metallic Cu catalysts in methanol synthesis. The Zn–Zn peak is much stronger for the 2:1 sample, thereby indicating the presence of ZnO nanocrystals; this is in good agreement with the XRD and the TEM results. In both cases, the coordination number of the Zn–Zn shell is much less than 12, which is the crystallographic coordination number of crystalline ZnO. We conclude that an appropriate concentration of Al_2O_3 can effectively disperse ZnO and inhibit the formation of crystalline ZnO.

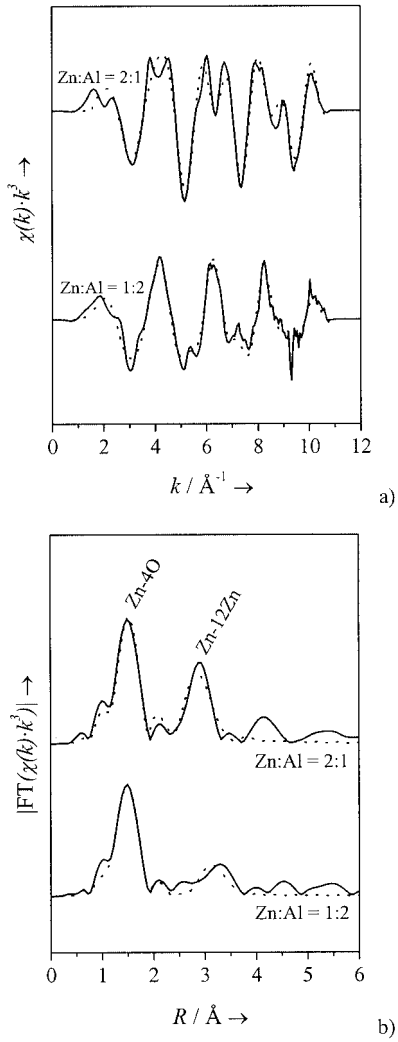

Figure 4. Zn K-edge EXAFS raw data (a) and Fourier transform magnitudes (b) of ZnO/Al_2O_3 calcined xerogels (400 °C) with different Zn/Al molar ratio. Solid line: experimental data; dotted line: fit data.

Nitrogen physisorption isotherms and the corresponding pore-size distributions of porous ZnO/Al_2O_3 samples are shown in Figure 5. The isotherms of both samples have significant hysteresis loops that are associated with the filling and emptying of mesopores by the condensate. ZnO/Al_2O_3 with a Zn/Al ratio of 1:2 has the smallest pore size and the narrowest distribution (Figure 5b). The pore sizes are in the range of 5–10 nm. With increasing Zn concentration, the pore size increases and the distribution is broadened considerably. When the Zn/Al ratio is 2:1 the pore sizes are in the range of 5–25 nm.

Table 1. Results of EXAFS fits of ZnO/Al_2O_3 calcined xerogels (Zn K-edge; 9659 eV).

Zn/Al molar ratio	R(Zn–O) [Å]	N(Zn–O)	σ^2(Zn–O) [$Å^2 \times 10^3$]	R(Zn–Zn) [Å]	N(Zn–Zn)	σ^2(Zn–Zn) [$Å^2 \times 10^3$]
1:2	1.95	3.5	7.7	3.52	0.6	1.97
2:1	1.96	3.7	6.1	3.21	7.3	13.2

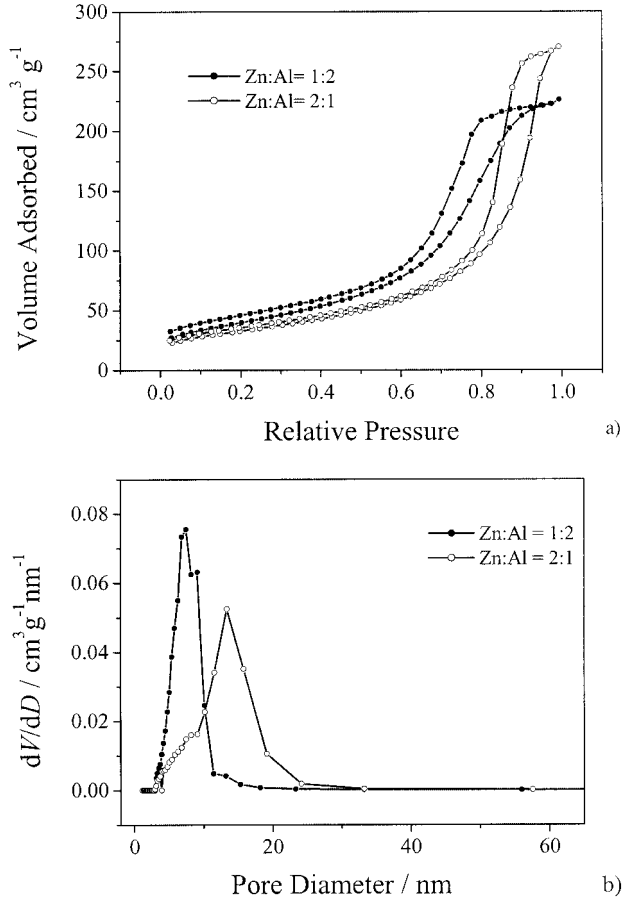

Figure 5. Nitrogen physisorption isotherms (a) and pore-size distribution (b) of ZnO/Al_2O_3 calcined xerogels (400 °C) with different Zn/Al ratios.

The BET surface area and the pore volume derived from nitrogen physisorption are listed in Table 2. An increase of the Zn concentration leads to a decrease of the BET surface area. A maximum surface area of 144 $m^2 g^{-1}$ was obtained for ZnO/Al_2O_3 with a Zn/Al ratio of 1:2, and this material also exhibits a smaller pore size and a narrower size distribution. The pore volume was found to be 0.42 $cm^3 g^{-1}$ for the sample with a Zn/Al ratio of 2:1. Baumann et al. have prepared Al_2O_3 aerogels by the same method and obtained a specific surface area of 289 $m^2 g^{-1}$, an average pore diameter of 32 nm, and pore volume of 2.6 $cm^3 g^{-1}$.[26] We conclude that the presence of Zn leads to smaller pores and a smaller specific surface area than with Al_2O_3 alone.

Table 2. BET surface area and pore volume of ZnO/Al_2O_3 calcined xerogels (400 °C).

Zn/Al molar ratio	BET surface area [$m^2 g^{-1}$]	Pore volume [$cm^3 g^{-1}$]
1:2	144	0.36
2:1	116	0.42

Copper-Containing Xerogels and Aerogels (Cu/Al and Cu/Zn/Al Systems)

The industrial catalyst in methanol synthesis contains metallic copper, zinc oxide, and aluminum oxide, therefore the synthesis was extended to copper as the third component. Xerogels were obtained by simple drying in air. Aerogels were also prepared with these systems to obtain samples with a high specific surface area. Supercritical point drying of the wet gels with CO_2 gave highly porous, fluffy materials with an effective density of about 0.9 $g cm^{-3}$. The aerogels are blue and then turn black after calcination at 400 °C. The Al_2O_3 phase is X-ray amorphous in both the calcined xerogels and the aerogels. The XRD patterns of both the CuO/Al_2O_3 and the $CuO/ZnO/Al_2O_3$ calcined xerogels show strong CuO peaks, as shown in Figure 6a, with ZnO as a crystalline phase in the latter case. The ZnO peaks are weak, thereby indicating a good dispersion and a small crystallite size. The decrease of the CuO peak intensities can be attributed to an improved dispersion due to the presence of ZnO. Compared to the calcined xerogels, the calcined aerogels exhibit weaker CuO and ZnO contributions characterized by broad peaks (Figure 6b). We conclude that the dispersions of both Cu and Zn are improved by the drying process with supercritical CO_2.

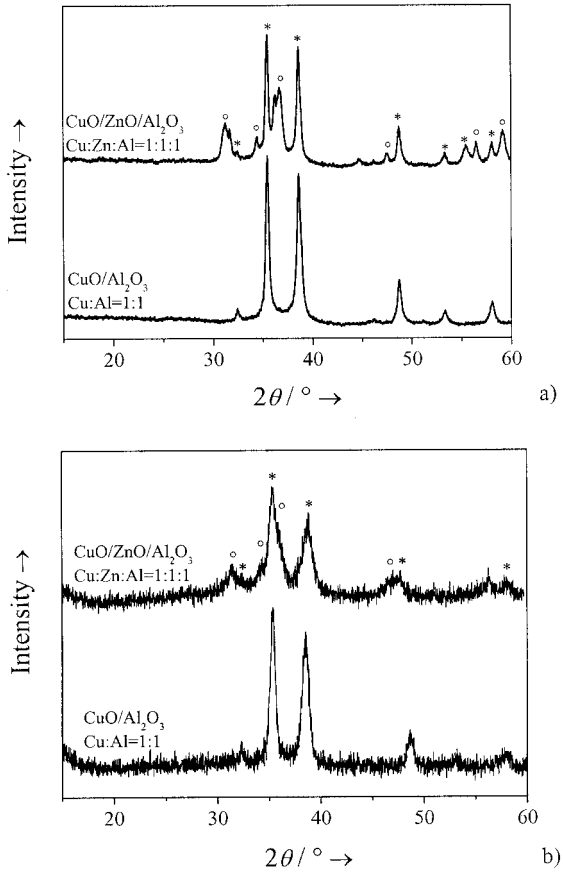

Figure 6. XRD patterns of CuO/Al_2O_3 and $CuO/ZnO/Al_2O_3$ calcined xerogels (a) and calcined aerogels (b). The marked peaks correspond to CuO (*) and ZnO (o), respectively.

Nitrogen physisorption of the CuO/Al_2O_3 and the $CuO/ZnO/Al_2O_3$ aerogels gave their pore-size distributions, which are broad in both cases (Figure 7). A narrow distribution in the range of 5–10 nm was obtained for the Zn/Al xerogel (see above). However, the Cu/Al aerogel gave a

distribution from 2 nm up to more than 30 nm. The presence of Zn narrows the pore-size distribution slightly and reduces the average pore size, as indicated by the shift of the peak maximum to smaller pore diameters.

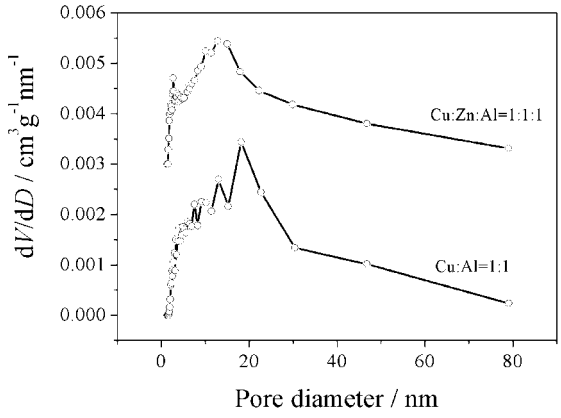

Figure 7. Pore-size distribution of CuO/Al_2O_3 and $CuO/ZnO/Al_2O_3$ calcined aerogels derived from nitrogen physisorption isotherms.

The CuO particle size and size distribution have a considerable influence on the reduction behavior.[30] For large CuO particles, the reduction of near-surface Cu^{II} species can occur at lower temperature.[31] The reduction of the bulk then appears at higher temperature. For small particles, the reduction may be very fast so that separate peaks or shoulders cannot be observed. In addition, the reduction behavior becomes even more complex due to the presence of $CuZnO_x$[32] and $CuAl_2O_4$.[33]

The TPR spectra of the calcined CuO/Al_2O_3 xerogels and aerogels are shown in Figure 8. In both samples the reduction of CuO occurs in three steps, presumably due to intermediate phases like Cu_2O[34] and the broad particle-size distribution. The first reduction step of the xerogel is characterized by a broad shoulder. The reduction starts at about 140 °C for both aerogel and xerogel. The peak maximum of the aerogel appears at 176 °C, a lower temperature than that of the xerogel, for which it appears at 220 °C. The shift of the peak to higher temperature can be attributed to an increased particle size of CuO. The reduction of the $CuO/ZnO/Al_2O_3$ xerogel occurs in two steps, as indicated by a peak and a shoulder on the left-hand side (Figure 8c), although the aerogel gave only one peak (Figure 8d). The peak maxima appear at 166 °C and 197 °C for the aerogel and xerogel, respectively. The reduction temperature is lower than those of the corresponding CuO/Al_2O_3 aerogel (176 °C) and xerogel (220 °C), which can be attributed to an increased dispersion of CuO. Obviously, ZnO plays a key role in the dispersion of CuO by increasing the metal–support interaction. The intermediate phases during the reduction are clearly different with or without ZnO, as reflected by the different reduction behaviors. The CuO contents of the samples were derived from the TPR spectra. The results were found to be in good agreement with the results obtained by AAS elemental analysis (Table 3). This confirms that the reduction of CuO during TPR is com-

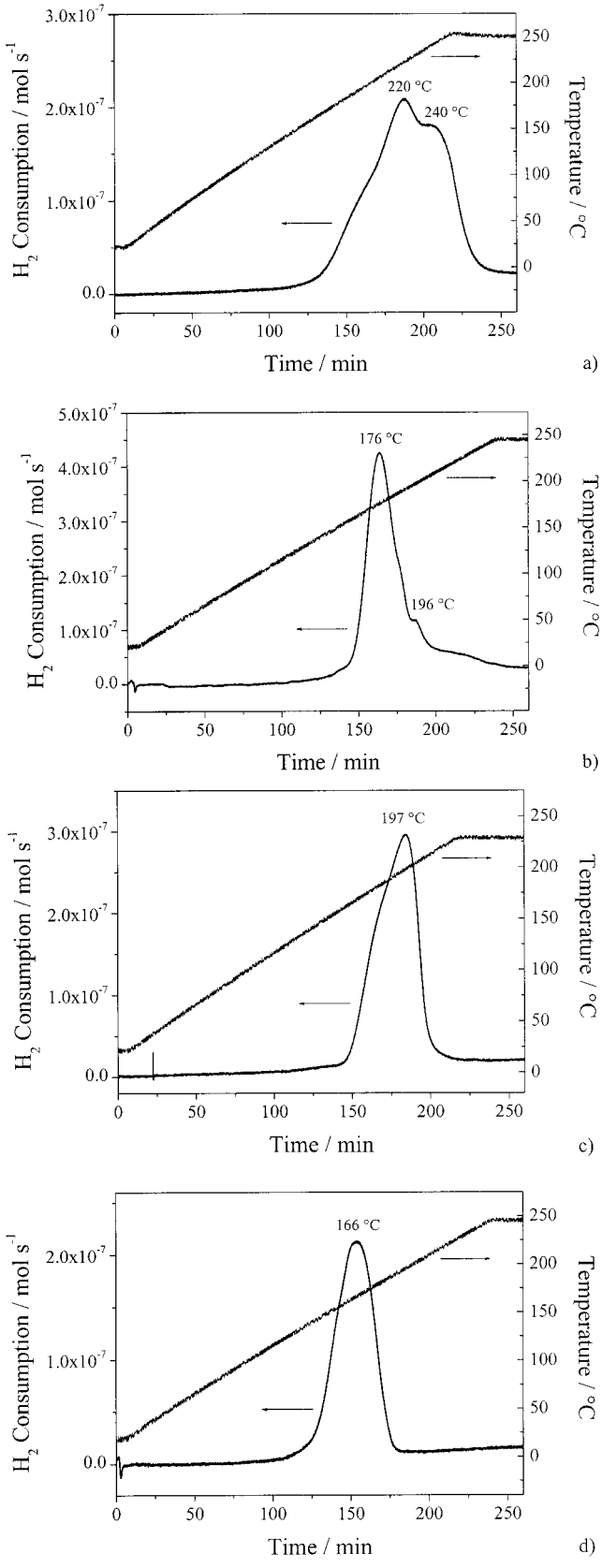

Figure 8. TPR patterns of CuO/Al_2O_3 (1:1) and $CuO/ZnO/Al_2O_3$ (1:1:1) calcined xerogels and aerogels at a heating rate of 1 K min^{-1} in H_2/He: a) CuO/ZnO (1:1) xerogel; b) CuO/ZnO (1:1) aerogel; c) $CuO/ZnO/Al_2O_3$ (1:1:1) xerogel; d) $CuO/ZnO/Al_2O_3$ (1:1:1) aerogel.

Table 3. CuO contents in the CuO/Al_2O_3 and $CuO/ZnO/Al_2O_3$ samples.

Samples	CuO/Al_2O_3 calcined xerogel	CuO/Al_2O_3 calcined aerogel	$CuO/ZnO/Al_2O_3$ calcined xerogel	$CuO/ZnO/Al_2O_3$ calcined aerogel
CuO [g_{cat}^{-1}]	Cu/Al = 1:1	Cu/Al = 1:1	Cu/Zn/Al = 1:1:1	Cu/Zn/Al = 1:1:1
by TPR	50.9 wt-%	52.7 wt-%	39.3 wt-%	34.2 wt-%
by AAS	50.4 wt-%	50.5 wt-%	38.6 wt-%	34.2 wt-%

Table 4. BET surface area, Cu surface area and catalytic activity for methanol synthesis of Cu/Zn/Al calcined xerogels and aerogels.

Sample		BET surface area [$m^2 g^{-1}$]	Pore volume [$cm^3 g^{-1}$]	Specific Cu surface area [$m^2 g^{-1}$]	Catalytic activity in methanol synthesis[a]
CuO/Al_2O_3	xerogel	34	–	3.7	2.0%
(Cu/Al = 1:1)	aerogel	222	1.03	5.2	4.0%
$CuO/ZnO/Al_2O_3$	xerogel	57	–	2.6	4.9%
(Cu/Zn/Al = 1:1:1)	aerogel	175	0.85	6.0	22%

[a] The activity of the industrial standard catalyst (ICI) was used as reference and set to 100%.

plete, and that the consumption of H_2 by other phases can be excluded.

Catalytic Activities of Cu-Containing Xerogels and Aerogels

The specific surface area of the samples was determined by nitrogen physisorption. Different drying methods (air or supercritical CO_2) have a significant influence on the surface area (Table 4). The porous microstructure of the wet gel is better preserved by supercritical drying, resulting in a higher specific surface area. High specific pore volumes (as much as 1 $cm^3 g^{-1}$) were found, compared to about 0.4 $cm^3 g^{-1}$ for the ZnO/Al_2O_3 calcined xerogel (Table 2). The specific Cu surface area,[4] as determined by N_2O reactive frontal chromatography, is given in Table 4. The higher Cu surface area of the Cu/Al or Cu/Zn/Al calcined xerogels leads to a higher catalytic activity, and both aerogels show a much higher activity in methanol synthesis than the corresponding xerogels. The presence of ZnO also improves the catalytic activities. In the 1:1 Cu/Al xerogels, the catalytic activity increases from 2.0% to 4.9% despite a smaller specific Cu surface area. The higher activity of the ternary aerogel can be attributed to a strong metal–support interaction, as supported by the XRD and TPR investigations. We note that the presence of Zn^{2+} or Cu^{2+} leads to a smaller specific surface area and a lower pore volume, but also to a smaller average pore size.

Conclusions

A sol–gel route has been employed to prepare Cu/Zn/Al xerogels and aerogels with propylene oxide as gelation initiator. ZnO can be atomically dispersed in Al_2O_3 in xerogels in a wide range of Zn concentrations. A higher Cu dispersion is found in the aerogels than in the xerogels, which leads to a higher specific surface area, a higher Cu surface area, and a higher catalytic activity in methanol synthesis. The presence of ZnO increases the catalytic activities in both the xerogel and aerogel, which we attribute to a strong metal–support interaction. The sol–gel method is easy to apply and well suited to the preparation of binary or ternary catalysts for methanol synthesis.

Experimental Section

Preparation of ZnO/Al_2O_3, CuO/Al_2O_3, and $CuO/ZnO/Al_2O_3$ Xerogels and Aerogels: $Cu(NO_3)_2 \cdot 3H_2O$ (Merck, 98%), $Zn(NO_3)_2 \cdot 6H_2O$ (Merck, 98%), and $Al(NO_3)_3 \cdot 9H_2O$ (Merck, 98%) were used as metal precursors, and propylene oxide (Acros, 99%) was used as gelation initiator.[20–22] Metal nitrates of different compositions were dissolved in absolute ethanol (typically 10–20 mL) to give a clear solution with a total metal ion concentration of 1 M. Propylene oxide was then added to the solution. The molar ratio of propylene oxide to the molar sum of the metal ions was 10:1. After stirring at room temperature for 10 min, the reaction mixture was transferred into a closed vessel. A wet gel formed within 30–60 min. This wet gel was allowed to age at room temperature for 24 h in the closed vessel and then soaked in a bath of absolute ethanol for 24 h to exchange the water from the pores of the gel. Note that the water is the water of crystallization of the starting salts. The exchange of water with ethanol was performed twice. The air-dried xerogel was then obtained by drying of the gel under air at room temperature for 5–6 d. For the preparation of an aerogel, the obtained wet gel was soaked in a bath of acetone for 24 h to exchange the ethanol and water from the pores. The exchange was repeated twice. A CO_2 critical point dryer (BAL-TEC, CPD 030) was then used to dry the wet gel. The acetone in the pores was extracted with liquid CO_2 6–8 times at 10 °C and 5.0 MPa. After that, the temperature was increased to 40 °C and the pressure to 7.5 MPa to give supercritical CO_2. The autoclave was then depressurized over about 1 h to give the aerogel. For calcination, the air-dried xerogel or aerogel was heated to 400 °C at a rate of 3 K min^{-1} under a dynamic air atmosphere in a tubular reactor to give an intimate mixture of CuO, ZnO, and Al_2O_3. The reactor was held at that temperature for 3 h, and then cooled to room temperature. After calcination, all copper-containing samples were black due to CuO formation and the other ones were white. Table 5 lists all prepared samples.

Table 5. Prepared samples of different compositions and molar ratios.

Xerogel	ZnO/Al_2O_3 Zn/Al = 2:1	ZnO/Al_2O_3 Zn/Al = 1:2	CuO/Al_2O_3 Cu/Al = 1:1	$CuO/ZnO/Al_2O_3$ Cu/Zn/Al = 1:1:1
Aerogel			CuO/Al_2O_3 Cu/Al = 1:1	$CuO/ZnO/Al_2O_3$ Cu/Zn/Al = 1:1:1

Characterization: Thermogravimetry was carried out with a Netzsch STA 409 TG-DTA/DSC instrument. Samples were heated from room temperature to 1000 °C at a rate of 5 K min^{-1} under dynamic O_2 atmosphere at a flow rate of 50 mL min^{-1}. The structure of the resulting products was studied by TEM with a Philips CM 200 FEG instrument. Powder XRD was carried out at room temperature in transmission mode at the B2 beamline at HASYLAB with monochromatic radiation or with a Siemens D5000 instrument with Cu-K_α radiation. EXAFS was carried out at the E4 beamline at HASYLAB/DESY in transmission mode at 77 K. The programs SPLINE and XFIT[35] were used for quantitative data evaluation. Theoretical standards were computed with the program FEFF 6.01a.[36] The amplitude reduction factor, S_o^2, was fixed to 1. Variation parameters were the bond lengths, the coordination numbers, the Debye–Waller factors (σ^2), and the zero-energy correction (E_o). The specific surface area was determined by nitrogen physisorption at 77 K (BET method). The pore-size distribution was obtained using the BJH method from the desorption branch of the isotherms. Temperature-programmed reduction (TPR) was carried out for the calcined xerogels and aerogels. About 0.1 g of the sample was placed in a quartz reactor. The reduction was performed under flowing diluted H_2 (4.2 vol-% H_2 in He) by increasing the temperature to 240 °C at 1 K min^{-1} and maintaining that temperature for 1 h. The active surface area of Cu was determined by N_2O reactive frontal chromatography at 300 K.[37] Atomic absorption spectroscopy (AAS) was performed with a Thermo Electron Corporation instrument (M series) to determine the copper content of the samples.

Catalytic Activity Measurements: Catalytic measurements were performed in a high-throughput 49-parallel channel reactor.[38] The catalyst (100 mg diluted with 200 mg of quartz per well) was placed in a sample holder consisting of a stainless-steel cartridge closed at the bottom by a stainless-steel sinter metal frit. Prior to the catalytic measurements, the catalysts were reduced with H_2 at 245 °C according to the procedure for the commercial benchmark catalyst ICI Katalco 51-8. Before measuring the catalytic activity, all samples were equilibrated for 3 h (reaction pressure: 4.5 MPa; reaction temperature: 245 °C; analytic flow: 20 mL min^{-1}). The reaction gas consisted of 70 vol-% H_2, 24 vol-% CO, and 6 vol-% CO_2. A double GC system (HP GC 6890) equipped with a methanizer FID was used for online gas analysis. Oxo product separation (H_3COH, $HCOOCH_3$, $H_3CCOOCH_3$, H_3CCH_2OH) was carried out on a SuppelcoWAX 0.53 mm column and CO, CO_2, and CH_4 were separated on a Carboxen 1006 column. Methanol productivities for all measured samples were compared to the productivity of the industrial benchmark catalyst ICI Katalco 51-8.

Acknowledgments

This work was supported by the Deutsche Forschungsgemeinschaft within the scope of the Collaborative Research Center SFB 558 ("Metal–substrate interactions in heterogeneous catalysis"). We thank HASYLAB at DESY (Hamburg) for generous allocation of synchrotron beam time. We thank F. Schüth, Mülheim/Ruhr, for helpful discussions and R. Naumann d'Alnoncourt for experimental assistance.

[1] C. Chauvin, J. Jaussey, J. C. Lavalley, H. Idriss, J. P. Hidermann, A. Kiennemann, P. Chaumette, P. Coutry, *J. Catal.* **1990**, *121*, 56–69.
[2] T. Ressler, B. L. Kniep, I. Kasatkin, R. Schlögl, *Angew. Chem.* **2005**, *117*, 4782–4785; *Angew. Chem. Int. Ed.* **2005**, *44*, 4704–4707.
[3] M. Saito, K. Murata, *Catal. Surv. Asia* **2004**, *8*, 285–294.
[4] G. E. Parris, K. Klier, *J. Catal.* **1986**, *97*, 374–384.
[5] P. L. Hansen, J. B. Wagner, S. Helveg, J. R. Rostrup-Nielsen, B. S. Clausen, H. Topsoe, *Science* **2002**, *295*, 2053–2055.
[6] J. B. Wagner, P. L. Hansen, A. M. Molenbroek, H. Topsoe, B. S. Clausen, S. Helveg, *J. Phys. Chem. B* **2003**, *107*, 7753–7758.
[7] R. Schlögl, *Angew. Chem.* **1993**, *105*, 403–405; *Angew. Chem. Int. Ed. Engl.* **1993**, *32*, 381–383.
[8] M. M. Günter, T. Ressler, B. Bems, C. Büscher, T. Genger, O. Hinrichsen, M. Muhler, R. Schlögl, *Catal. Lett.* **2001**, *71*, 37–44.
[9] B. Bems, M. Schur, A. Dassenoy, H. Junkes, D. Herein, R. Schlögl, *Chem. Eur. J.* **2003**, *9*, 2039–2052.
[10] H. Wilmer, M. Kurtz, K. Klementiev, O. Tkachenko, W. Grünert, O. Hinrichsen, A. Birkner, S. Rabe, K. Merz, M. Driess, C. Wöll, M. Muhler, *Phys. Chem. Chem. Phys.* **2003**, *5*, 4736–4742.
[11] B. L. Kniep, T. Ressler, A. Rabis, F. Girgsdies, M. Baenitz, F. Steglich, R. Schlögl, *Angew. Chem.* **2004**, *116*, 114–117; *Angew. Chem. Int. Ed.* **2004**, *43*, 112–115.
[12] M. Schur, B. Bems, A. Dassenoy, I. Kassatkine, J. Urban, H. Wilmes, O. Hinrichsen, M. Muhler, R. Schlögl, *Angew. Chem.* **2003**, *115*, 3945–3947; *Angew. Chem. Int. Ed.* **2003**, *42*, 3815–3817.
[13] M. Kurtz, H. Wilmer, T. Genger, O. Hinrichsen, M. Muhler, *Catal. Lett.* **2003**, *86*, 77–80.
[14] D. Fang, Z. Liu, Y. Yang, H. Zhang, J. Lin, *Shiyou Huagong* **2005**, *34*, 1032–1037; *Chem. Abstr.* **2006**, *145*, 175100.
[15] J. F. Deng, Q. Sun, Y. L. Zhang, S. Y. Chen, D. Wu, *Appl. Catal. A* **1996**, *139*, 75–85.
[16] J. Hambrock, M. K. Schroeter, A. Birkner, C. Woell, R. A. Fischer, *Chem. Mater.* **2003**, *15*, 4217–4222.
[17] S. Vukojević, O. Trapp, J. D. Grunwaldt, C. Kiener, F. Schüth, *Angew. Chem.* **2005**, *117*, 8192–8195; *Angew. Chem. Int. Ed.* **2005**, *44*, 7978–7981.
[18] Y. Guo, R. Weiss, M. Epple, *Eur. J. Inorg. Chem.* **2005**, 3072–3079.
[19] Y. Guo, R. Weiss, R. Boese, M. Epple, *Thermochim. Acta* **2006**, *446*, 101–105.
[20] R. Weiss, G. Jansen, R. Boese, M. Epple, *Dalton Trans.* **2006**, 1831–1835.
[21] R. Weiss, Y. Guo, S. Vukojević, L. Khodeir, R. Boese, F. Schüth, M. Muhler, M. Epple, *Eur. J. Inorg. Chem.* **2006**, 1796–1802.
[22] C. J. Brinker, G. W. Scherer, *Sol–Gel Science. The Physics and Chemistry of Sol–Gel Processing*, Academic Press, Boston, **1990**.
[23] J. Livage, M. Henry, C. Sanchez, *Prog. Solid State Chem.* **1988**, *18*, 259–341.
[24] A. E. Gash, T. M. Tillotson, J. H. Satcher, J. F. Poco, L. W. Hrubesh, R. L. Simpson, *Chem. Mater.* **2001**, *13*, 999–1007.
[25] A. E. Gash, T. M. Tillotson, J. H. Satcher Jr, L. W. Hrubesh, R. L. Simpson, *J. Non-Cryst. Solids* **2001**, *285*, 22–28.
[26] T. F. Baumann, A. E. Gash, S. C. Chinn, A. M. Sawvel, R. S. Maxwell, J. H. Satcher Jr, *Chem. Mater.* **2005**, *17*, 395–401.
[27] A. E. Gash, J. H. Satcher, R. L. Simpson, *Chem. Mater.* **2003**, *15*, 3268–3275.

[28] C. N. Chervin, B. J. Clapsaddle, H. W. Chiu, A. E. Gash, J. H. Satcher Jr, S. M. Kauzlarich, *Chem. Mater.* **2005**, *17*, 3345–3351.
[29] H. K. Cammenga, M. Epple, *Angew. Chem.* **1995**, *107*, 1284–1301; *Angew. Chem. Int. Ed. Engl.* **1995**, *34*, 1171–1187.
[30] J. Agrell, K. Hasselbo, K. Jansson, S. G. Järas, M. Boutonnet, *Appl. Catal. A* **2001**, *221*, 239–250.
[31] M. Turco, G. Bagnasco, U. Costantino, F. Marmottini, T. Montanari, G. Ramis, G. Busca, *J. Catal.* **2004**, *228*, 43–55.
[32] H. Wilmer, T. Genger, O. Hinrichsen, *J. Catal.* **2003**, *215*, 188–198.
[33] S. Velu, K. Suzuki, M. Okazaki, M. P. Kapoor, T. Osaki, F. Ohashi, *J. Catal.* **2000**, *194*, 373–384.
[34] M. M. Günter, T. Ressler, R. E. Jentoft, B. Bems, *J. Catal.* **2001**, *203*, 133–149.
[35] P. J. Ellis, H. C. Freeman, *J. Synchrotron Radiat.* **1995**, *2*, 190–195.
[36] E. A. Stern, M. Newville, B. Ravel, Y. Yacoby, D. Haskel, *Physica B* **1995**, *208–209*, 117–120.
[37] O. Hinrichsen, T. Genger, M. Muhler, *Chem. Eng. Technol.* **2000**, *11*, 956–959.
[38] C. Kiener, M. Kurtz, H. Wilmer, C. Hoffmann, H. W. Schmidt, J. D. Grunwaldt, M. Muhler, F. Schüth, *J. Catal.* **2003**, *216*, 110–119.

Received: June 14, 2006
Published Online: October 12, 2006

